



**HAL**  
open science

## Role of near-infrared fluorescence imaging in the resection of metastatic lymph nodes in an optimized orthotopic animal model of HNSCC

I. Atallah, C. Milet, R. Quatre, M. Henry, E. Reyt, J.-L. Coll, A. Hurbin, C.A. Righini

### ► To cite this version:

I. Atallah, C. Milet, R. Quatre, M. Henry, E. Reyt, et al.. Role of near-infrared fluorescence imaging in the resection of metastatic lymph nodes in an optimized orthotopic animal model of HNSCC. *European Annals of Otorhinolaryngology, Head and Neck Diseases*, 2015, 132 (6), pp.337-342. 10.1016/j.anorl.2015.08.022 . hal-02349440

**HAL Id: hal-02349440**

**<https://hal.science/hal-02349440>**

Submitted on 5 Nov 2019

**HAL** is a multi-disciplinary open access archive for the deposit and dissemination of scientific research documents, whether they are published or not. The documents may come from teaching and research institutions in France or abroad, or from public or private research centers.

L'archive ouverte pluridisciplinaire **HAL**, est destinée au dépôt et à la diffusion de documents scientifiques de niveau recherche, publiés ou non, émanant des établissements d'enseignement et de recherche français ou étrangers, des laboratoires publics ou privés.



Available online at  
**ScienceDirect**  
[www.sciencedirect.com](http://www.sciencedirect.com)

Elsevier Masson France  
**EM|consulte**  
[www.em-consulte.com/en](http://www.em-consulte.com/en)



Original article

# Role of near-infrared fluorescence imaging in the resection of metastatic lymph nodes in an optimized orthotopic animal model of HNSCC

I. Atallah<sup>a,\*,b,c</sup>, C. Milet<sup>b,c</sup>, R. Quatre<sup>a,b,c</sup>, M. Henry<sup>b,c</sup>, E. Reyt<sup>a,b</sup>, J.-L. Coll<sup>b,c</sup>,  
A. Hurbin<sup>b,c,1</sup>, C.A. Righini<sup>a,b,c,1</sup>

<sup>a</sup> Clinique universitaire d'ORL, CHU de Grenoble, BP 217, 38043 Grenoble cedex 9, France

<sup>b</sup> Université Joseph-Fourier, BP 53, 38041 Grenoble cedex 9, France

<sup>c</sup> Unité Inserm U823, institut Albert-Bonniot, BP 170, 38042 Grenoble cedex 9, France

## ARTICLE INFO

### Keywords:

Near-infrared fluorescence imaging-guided surgery  
Head and neck squamous cell carcinoma  
Metastatic adenopathy  
 $\alpha v \beta 3$  integrin  
RAFT-c(RGD)<sub>4</sub>

## ABSTRACT

**Objectives:** To study the role of near-infrared fluorescence imaging in the detection and resection of metastatic cervical lymph nodes in head and neck cancer.

**Materials and methods:** CAL33 head and neck cancer cells of human origin were implanted in the oral cavity of nude mice. The mice were followed up after tumor resection to detect the development of lymph node metastases. A specific fluorescent tracer for  $\alpha v \beta 3$  integrin expressed by CAL33 cells was injected intravenously in the surviving mice between the second and the fourth month following tumor resection. A near-infrared fluorescence-imaging camera was used to detect tracer uptake in metastatic cervical lymph nodes, to guide of lymph-node resection for histological analysis.

**Results:** Lymph node metastases were observed in 42.8% of surviving mice between the second and the fourth month following orthotopic tumor resection. Near-infrared fluorescence imaging provided real-time intraoperative detection of clinical and subclinical lymph node metastases. These results were confirmed histologically.

**Conclusion:** Near infrared fluorescence imaging provides real-time contrast between normal and malignant tissue, allowing intraoperative detection of metastatic lymph nodes. This preclinical stage is essential before testing the technique in humans.

© 2015 Elsevier Masson SAS. All rights reserved.

## 1. Introduction

In head and neck squamous cell carcinoma (HNSCC), surgery should achieve complete resection with adequate safe margins. In addition to tumor resection, given the rate of lymph-node invasion in HNSCC, which can be as high as 30% to 40% in patients without any clinical adenopathy (cNO), neck dissection should in principle be associated, for both diagnostic and therapeutic purposes. It should be as complete as possible and should include all the lymph-node areas in the lymphatic drainage territory of the primary tumor. In the literature there are few techniques allowing real-time intraoperative detection of metastatic lymph nodes. Such

techniques should optimize neck dissection by making it selective, with only metastatic adenopathies being resected.

Near-infrared fluorescence imaging for diagnosis, treatment and follow-up of HNSCC is a fast developing field. It provides real-time information on the localization and extension of malignant tissue through creation of a specific contrast between normal and cancer tissue. It requires fluorescent probes that specifically target cancer cells. One of the most important targets is  $\alpha v \beta 3$  integrin, which is widely expressed on the surface of tumor-vessel endothelial cells and by most tumor cells, including HNSCC, during migration or by cells located on invasion frontlines [1–3]. Previous studies showed that near-infrared fluorescence imaging targeting  $\alpha v \beta 3$  integrin provides benefit in HNSCC surgery by improving resection quality through the detection of tumor residue within the surgical bed that would be invisible to the naked eye even under magnifying lenses, so that the residue would be overlooked in purely macroscopically guided resection. It was further demonstrated that this detection of cancer residues positively impacted recurrence-free survival in an

\* Corresponding author.

E-mail address: [IAtallah@chu-grenoble.fr](mailto:IAtallah@chu-grenoble.fr) (I. Atallah).

<sup>1</sup> The two authors contributed equally to the study.

orthotopic animal model of HNSCC, which was developed by our team [4,5].

The present study examined the role of near-infrared fluorescence imaging in the detection and resection of metastatic cervical adenopathies in our orthotopic animal model of HNSCC. We injected a fluorescent peptide specific for  $\alpha v\beta 3$  integrin in order to target cancer cells within adenopathies. This targeting was visualized by a near-infrared fluorescence-imaging device that was previously miniaturized and specifically adapted for future applications in HNSCC surgery.

## 2. Material and methods

### 2.1. Cell line

In our experiments, we used the CAL33 HNSCC cell line, supplied free of charge by the Antoine Lacassagne Cancer Center oncopharmacology laboratory, Nice (France). It was established from a tissue sample taken from a human oral cavity moderately differentiated malpighian carcinoma [6], and showed stable expression of luciferase gene by lentiviral transfection, allowing *in vivo* bioluminescence imaging to detect lymph-node metastases. Cells were kept in Dulbecco's modified Eagle's medium (DMEM) with 10% fetal calf serum in a humid incubator at 37 °C and an atmosphere containing 5% CO<sub>2</sub>.

### 2.2. Molecular targeting

AngioStamp™ 800 (Fluoptics, Grenoble, France) is a peptide coupled to a fluorophore. It shows specific binding to  $\alpha v\beta 3$  integrin. It has a maximal absorbance at 781 nm and maximal emission at 794 nm. It was injected intravenously into the mouse tail under an inhaled general anesthesia, at 10 nmol per mouse 16–24 hours before fluorescence acquisition. The *in vivo* fluorescent signal was acquired by the near-infrared fluorescence imaging system described below.

### 2.3. Near-infrared fluorescence imaging system

FluoStick™ (Fluoptics, Grenoble, France) is a small-diameter imaging system, miniaturized and specifically adapted for future applications in HNSCC surgery [5]. It is intended for intraoperative fluorescence imaging using fluorophores with maximal absorbance around 770 nm and maximal emission around 820 nm.

### 2.4. Orthotopic animal HNSCC model

The animals used in the study were female nude mice aged 5–6 weeks, from Janvier Labs (Le Genest, Saint-Isle, France). The experimental protocol was approved by the French Education and Research Ministry (experimentation authorization no. 00392.02).

The orthotopic HNSCC model was previously described and validated [4,5]. Briefly, a 0.5–1 mm tumor fragment from tumor developing secondarily to subcutaneous CAL33 cell implantation in adult mice was implanted in the inner aspect of the animal's cheek ( $n = 14$ ). Once developed, the tumor was completely resected through an external incision of the cheek, under near-infrared fluorescence imaging after intravenous injection of AngioStamp™ 800. Mice were followed up for 6 months post-explantation to detect late tumor recurrence and lymph-node metastasis through bioluminescence imaging which is described below, then sacrificed at end of follow-up or onset of tumor recurrence or clinical or subclinical lymph-node metastasis; weight-loss exceeding 15% and general health deterioration also led to sacrifice.

### 2.5. Bioluminescence imaging

*In vivo* bioluminescence imaging was used to track tumor growth and detect recurrence and/or metastatic adenopathies. Five minutes before acquisition, intraperitoneal luciferin injection (150 mg/kg) was performed and then animals were kept under general inhaled anesthesia (isoflurane 4% for induction and 1.5% for maintenance) during bioluminescence acquisition on the IVIS Kinetic system (Caliper Life Sciences).

### 2.6. Lymph-node surgery

When metastatic adenopathy was detected, AngioStamp™ 800 was injected intravenously at 10 nmol per injection. Mice were anesthetized with isoflurane 4% for induction and 1.5% for maintenance; 16–24 hours after injection, a fluorescence acquisition was taken before and after wide cervical incision exposing all the anatomic structures of the neck. Mice were then sacrificed by cervical dislocation. Suspect adenopathies and adenopathies showing fluorescent signal were resected and analyzed histologically. Control lymph nodes (unsuspicious, non-fluorescent) were also excised and analyzed.

### 2.7. Hematoxylin-eosin (H&E) staining

Lymph-node tumor cell detection was performed on histologic slices with H&E staining. Samples were fixed in 4% PFA, dehydrated in successively increasing alcohol baths, then included in paraffin and sliced by microtome with 7  $\mu$ m thickness. Slices were deparaffinized in xylene baths, rehydrated in successively decreasing alcohol baths, then stained with hematoxylin for 4 minutes and rinsed in flowing water, stained with eosin for 2 minutes and rinsed again in flowing water. The stained slices were fixed in 100% ethanol then xylene, and slide mounted for histology under a BX41 Olympus microscope.

## 3. Results

### 3.1. Development of an orthotopic model of lymph-node metastasis in HNSCC

Fourteen mice with orthotopic HNSCC underwent complete near-infrared fluorescence-guided resection and were then followed up for 6 months on bioluminescence imaging to detect tumor recurrence or metastatic adenopathy. Four mice (28.5%) had local recurrence during the first 2 months. During the following 4 months, 3 mice showed signs of deteriorated general health status with >15% weight loss, without recurrence or detectable metastatic adenopathy, and were sacrificed. Bioluminescence detected metastatic adenopathy (Fig. 1) in 3 of the 7 surviving mice (42.8%) between the 3rd and 5th month post-implantation (2nd to 4th month after orthotopic tumor explantation). When the adenopathies were large, they were also detectable macroscopically and on palpation. Histologic analysis of resected suspicious lymph nodes found metastasis of malpighian carcinoma (Fig. 2A).

### 3.2. Near-infrared fluorescence imaging guided lymph-node surgery in HNSCC

The detected metastatic adenopathies were sampled by near-infrared fluorescence-guided surgery after AngioStamp™ 800 injection. In the absence of clinically detectable metastatic adenopathy, preoperative bioluminescence imaging and pre- and intra-operative fluorescence imaging showed no cervical fluorescent signal (Fig. 3A). Histologic analysis of a sampled control lymph node found no abnormality (Fig. 3A, yellow arrow). Conversely,

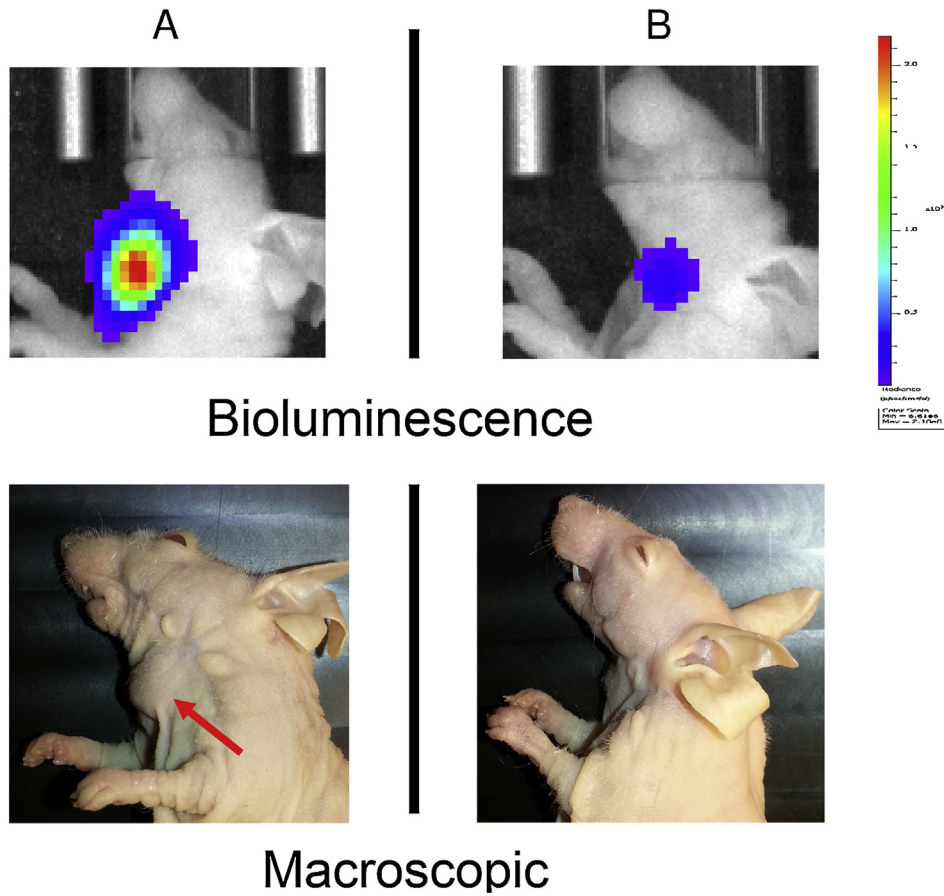


**Fig. 1.** Detection of metastatic adenopathies. Metastatic lymph nodes could be either detected on bioluminescence imaging or macroscopically (A). In some cases, metastatic lymph nodes are only detected by bioluminescence imaging (B).

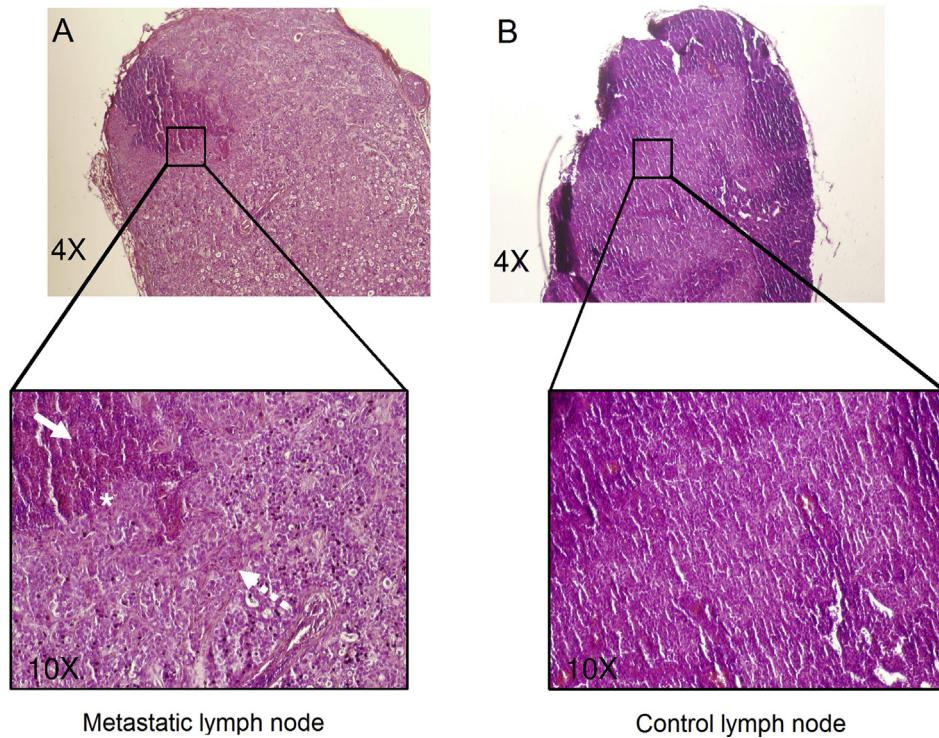


**Fig. 2.** Histologic (H&E) lymph-node analysis. A. In metastatic adenopathy, squamous cell carcinoma (dotted arrow) infiltrates almost the entire lymph node; note also the interface (star) between residual lymphocyte population (arrow) and metastasis. B. Control lymph node, showing a structure free of any tumor invasion.

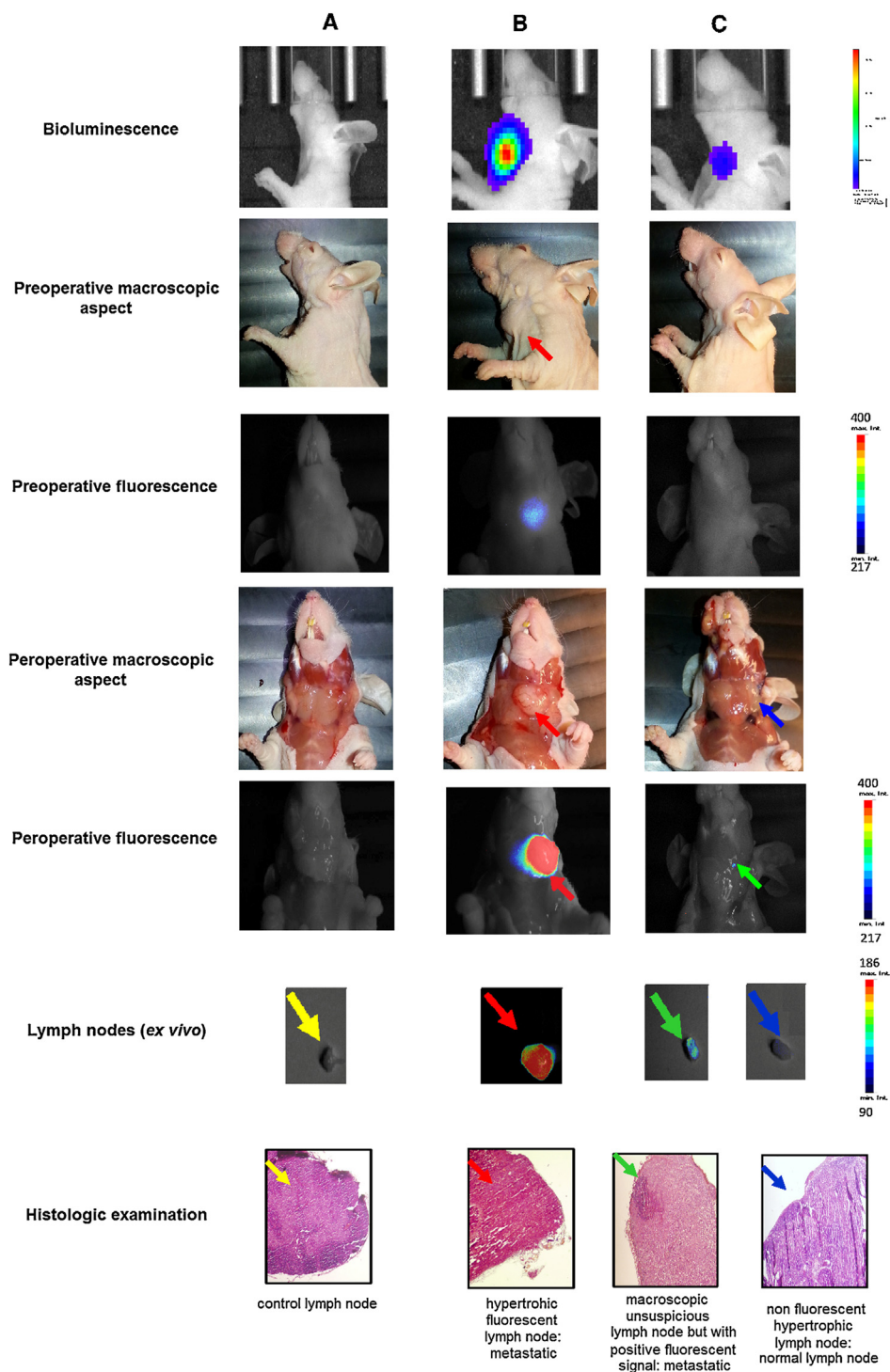


**Figure 3.** Contribution of near-infrared fluorescence imaging in HNSCC lymph-node surgery. Mouse A presents no detectable metastatic adenopathy on macroscopic examination, bioluminescence imaging or fluorescence imaging. Mouse B presents a metastatic adenopathy macroscopically detectable as well as on pre- and intra-operative bioluminescence and fluorescence imaging; pathologic analysis confirmed the metastatic character of the adenopathy (red arrow). Mouse C presents a cervical bioluminescent signal, but no adenopathy is detectable preoperatively. Intra-operatively, a hypertrophic adenopathy (blue arrow) shows no fluorescent signal; in contrast, an unsuspecting lymph node does show a fluorescent signal (green arrow). Both adenopathies were sampled for histology and compared with a control lymph node. The fluorescent adenopathy showed metastasis of squamous cell carcinoma, while the macroscopically suspicious non-fluorescent adenopathy and control lymph node showed no abnormality on histologic analysis.

in case of macroscopically detectable preoperative adenopathy (Fig. 3B, red arrow) associated with a bioluminescence signal, a fluorescent signal was also observed on pre- and intra-operative fluorescence imaging (Fig. 3B, red arrow). Histologic analysis of the hypertrophied fluorescent lymph node demonstrated metastasis (Fig. 3B, red arrow). Finally, in case of adenopathy with

preoperative bioluminescence signal but macroscopically undetectable due to lack of morphological signs of malignancy (Fig. 3C), a signal was observed only on intraoperative fluorescence imaging (Fig. 3C, green arrow). This lymph node did not seem suspicious on intraoperative macroscopic examination, unlike another hypertrophied but non-fluorescent node (Fig. 3C, blue arrow). Histologic

analysis showed the fluorescent adenopathy to be metastatic (Fig. 3C, green arrow) and the hypertrophied non-fluorescent node, like a control node, to be normal (Fig. 3C, blue and yellow arrows). The results of near-infrared fluorescence imaging-guided lymph-node surgery demonstrated that fluorescence imaging effectively guided intraoperative sampling of metastatic lymph nodes, even when clinically undetectable.

#### 4. Discussion

Development and assessment of new diagnostic and therapeutic tools for HNSCC require prior testing in a suitable animal model, which needs to be reproducible and representative of HNSCC. In a previous study, our team developed an orthotopic animal model of HNSCC, with 30 days' survival with *in situ* tumor. We opted for oral cavity implantation of tumor fragments rather than directly injecting tumor cells [5]. In other orthotopic models described in the literature, cell injection may induce dissemination of cancer cells by the hydrostatic pressure from the syringe during injection, resulting in the rapid development of large tumors, requiring sacrifice and thus making it difficult for lymph-node metastasis to develop [7–9]. In certain orthotopic animal HNSCC models using cell injection, the cervical lymph-node metastases that did develop may have been due to cell dissemination by hydrostatic pressure in the lymph vessels during injection rather than to cell migration from the primary site [9,10]. Such models thus fail to reproduce the reality of the lymph-node metastasis process. The present orthotopic animal model of HNSCC allowed tumor resection without sacrifice, and thus long follow-up to detect tumor recurrence and the development of metastatic adenopathy. The present study demonstrated that the model allowed metastatic adenopathy to develop in 42.8% of mice between the 2nd and 4th month after tumor resection, a percentage approximating the 30–40% rate of lymph-node invasion in human HNSCC. The model thus faithfully represents all characteristics of HNSCC, enabling the impact of new surgical or medical techniques on the primary site and on metastatic adenopathy to be assessed.

Several strategies have been suggested for fluorescence imaging-guided HNSCC surgery. Clinical application requires pharmacokinetic study of each new fluorescent probe. Indocyanine green (ICG) was one of the first fluorophores tested in near-infrared fluorescence-guided HNSCC surgery and proved effective in detecting sentinel nodes. It shows passive drainage by the lymphatic system. Rather than specifically targeting cancer tissue, ICG is taken up by the enhanced permeability and retention (EPR) effect [7], in which the large diameter of endothelial fenestration, hemodynamic changes within tumoral neovessels and the low level of lymphatic drainage of tumors leads to an accumulation of particles and small agents in the tumor tissue. ICG is thus not useful for optimizing HNSCC resection margins or detecting lymph-node metastasis [11–13]. Fluorescent probes specifically targeting receptors expressed by HNSCC, in contrast, provide real-time distinction between cancerous and healthy tissue.

One of the most important targets of fluorescent probes in oncology is  $\alpha v\beta 3$  integrin, which shows large expression in neovessels and certain tumors, including HNSCC [1–3]. It plays an important role in angiogenesis, cell proliferation and migration and metastasis. Among probes targeting  $\alpha v\beta 3$ , the RAFT-c(-RGDfK-)<sub>4</sub> (regioselectively addressable functionalized template-arginine-glycine-aspartic acid) peptide showed specificity *in vitro* and *in vivo* and has been coupled to many fluorophores to create specific fluorescent probes such as AngioStamp™ 800, used in the present study [14–16].

The present study confirmed previous findings in the optimization of tumor resection under near-infrared fluorescence

imaging. The local recurrence rate was 28.5% in the first 2 months after resection, in agreement with our previous rate of  $25 \pm 5\%$  [5]. AngioStamp™ 800 was also injected intravenously in surviving mice between the 2nd and 4th month post-explantation. Near-infrared fluorescence imaging detected clinically observed adenopathies but also those undetectable macroscopically pre- or intra-operatively; their metastatic character was confirmed by histology. In mice with cervical adenopathies on clinical examination and/or with bioluminescent cervical signal, near-infrared fluorescence imaging was thus able to confirm metastatic status. Intra-operatively, it also helps the surgeon remove a targeted metastatic adenopathy that is undetectable pre- or intra-operatively. Real-time near-infrared fluorescence imaging thus provides real benefit, specifically in HNSCC, guiding neck dissection so as exhaustively to resect metastatic cervical adenopathies and optimize neck dissection.

#### 5. Conclusion

Near-infrared fluorescence imaging is a promising and precious tool in HNSCC surgery. As well as improving tumor resection quality in the present orthotopic animal mode, it guided resection of clinically unidentifiable metastatic adenopathies. The present pre-clinical study is indispensable before human trials.

#### Disclosure of interest

The authors declare that they have no conflicts of interest concerning this article.

#### Acknowledgments

Thanks to the Groupe Pasteur mutualité fondation d'entreprise, the French Society of ORL (SFORL) and the Avenir Foundation for financial support, and to Fluoptics (Grenoble, France) for technical help.

#### References

- [1] Fabricius EM, Wildner GP, Kruse-Boitschenko U, et al. Immunohistochemical analysis of integrins  $\alpha v\beta 3$ ,  $\alpha v\beta 5$  and  $\alpha 5\beta 1$ , and their ligands, fibrinogen, fibronectin, osteopontin and vitronectin, in frozen sections of human oral head and neck squamous cell carcinomas. *Exp Ther Med* 2011;2:9–19.
- [2] Beer AJ, Grosu AL, Carlsen J, et al. [<sup>18F</sup>]galacto-RGD positron emission tomography for imaging of  $\alpha v\beta 3$  expression on the neovasculature in patients with squamous cell carcinoma of the head and neck. *Clin Cancer Res* 2007;13:6610–6.
- [3] Li P, Liu F, Sun L, et al. Chemokine receptor 7 promotes cell migration and adhesion in metastatic squamous cell carcinoma of the head and neck by activating integrin  $\alpha v\beta 3$ . *Int J Mol Med* 2011;27:679–87.
- [4] Atallah I, Milet C, Coll JL, et al. Role of near-infrared fluorescence imaging in head and neck cancer surgery: from animal models to humans. *Eur Arch Otorhinolaryngol* 2015;272(10):2593–600.
- [5] Atallah I, Milet C, Henry M, et al. Near-infrared fluorescence imaging-guided surgery improves the recurrence-free survival rate in a novel orthotopic animal model of HNSCC. *Head Neck* 2014.
- [6] Gioanni J, Fischel JL, Lambert JC, et al. Two new human tumor cell lines derived from squamous cell carcinomas of the tongue: establishment, characterization and response to cytotoxic treatment. *Eur J Cancer Clin Oncol* 1988;24:1445–50.
- [7] Keerweer S, Mol IM, Kerrebijn JD, et al. Targeting integrins and enhanced permeability and retention (EPR) effect for optical imaging of oral cancer. *J Surg Oncol* 2012;105:714–8.
- [8] Bozec A, Sudaka A, Toussan N, et al. Combination of sunitinib, cetuximab and irradiation in an orthotopic head and neck cancer model. *Ann Oncol* 2009;20:1703–10.
- [9] Gleysteen JP, Newman JR, Chhieng D, et al. Fluorescent labeled anti-EGFR antibody for identification of regional and distant metastasis in a preclinical xenograft model. *Head Neck* 2008;30:782–9.
- [10] Day KE, Sweeny L, Kulbersh B, et al. Preclinical comparison of near-infrared-labeled cetuximab and panitumumab for optical imaging of head and neck squamous cell carcinoma. *Mol Imaging Biol* 2013;15:722–9.

- [11] Gioux S, Choi HS, Frangioni JV. Image-guided surgery using invisible near-infrared light: fundamentals of clinical translation. *Mol Imaging* 2010;9:237–55.
- [12] Gibbs SL. Near infrared fluorescence for image-guided surgery. *Quant Imaging Med Surg* 2012;2:177–87.
- [13] van der Vorst JR, Schaafsma BE, Verbeek FP, et al. Near-infrared fluorescence sentinel lymph node mapping of the oral cavity in head and neck cancer patients. *Oral Oncol* 2013;49:15–9.
- [14] Jin ZH, Josserand V, Razkin J, et al. Noninvasive optical imaging of ovarian metastases using Cy5-labeled RAFT-c(-RGDFK)-4. *Mol Imaging* 2006;5:188–97.
- [15] Jin ZH, Josserand V, Foillard S, et al. In vivo optical imaging of integrin alphaV-beta3 in mice using multivalent or monovalent cRGD targeting vectors. *Mol Cancer* 2007;6:41.
- [16] Sancey L, Ardisson V, Riou LM, et al. In vivo imaging of tumour angiogenesis in mice with the alpha(v)beta (3) integrin-targeted tracer <sup>99m</sup>Tc-RAFT-RGD. *Eur J Nucl Med Mol Imaging* 2007;34:2037–40.